International Journal of Non-Linear Mechanics 118 (2020) 103286

Contents lists available at ScienceDirect

International Journal of Non-Linear Mechanics

journal homepage: www.elsevier.com/locate/nlm

A total Lagrangian elasticity formulation for the nonlinear free vibration of anisotropic beams

Paul R. Heyliger *, Abdullah Asiri

Department of Civil Engineering, Colorado State University, Fort Collins, CO 80523, United States of America

A B S T R A C T

The large amplitude free vibration response of isotropic and anisotropic beams is considered using a total Lagrangian description of the motion along with Ritz-based approximations to the dynamic statement of virtual work. Results are presented for both axial and bending modes and are compared with existing results in the literature using various formulations along with a finite element solution of the Euler–Bernoulli beam with Föppl–von Karman nonlinearity. Results from the present formulation include all nonlinear strain terms and give frequency ratios that are in excellent agreement with both Euler–Bernoulli and higher order beam theories for slender beams under small amplitudes but grow noticeably higher than those of other beam models as the beam becomes thick and the amplitude of vibration increases.

1. Introduction

The nonlinear vibration of beams has been studied for decades. For the most elementary description of the axial deformation of bars and the transverse motion of slender beams, the second-order ordinary differential equation that represents the former and the fourth-order ordinary differential equation that models the latter using Euler–Bernoulli theory [1] that are usually uncoupled for linear analysis now become coupled and must be solved simultaneously. Depending on support conditions, the axial force that can be generated within the beam tends to stiffen the beam as it deforms and hence the bending stiffness and resulting frequencies of vibration tend to increase as the relative magnitude of the deformation increases. The first study to capture this effect was completed in 1950 by Woinowsky–Krieger [2], and was followed by several other studies in the years to follow. Burgreen [3] and Ray and Bert [4] both studied nonlinear vibrations of beams with pinned ends and Srinivasan [5] extended many of these concepts to include beams and plates. Evenson [6] considered nonlinear beam vibrations for a variety of end conditions, and related studies were completed by Prathap and Varadan [7], Bhashyam and Prathap [8], and Reddy and Singh [9]. A number of finite element approaches were developed for nonlinear beam vibration included those of Sarma and Varadan [10,11]. Most of these studies focused on Euler–Bernoulli descriptions of beam bending, although Timoshenko theory was used by Sarma and Varadan [12]. A higher-order beam theory was used by Heyliger and Reddy [13] that incorporated shear deformation without the use of a shear coefficient. Several nonlinear beam models for straight and curved beams have been given by Pai and Nayfeh [14], Mayo and co-workers [15], Hodges and co-workers [16], and Lewandowski [17]. Ribeiro and Peyt [18] and Ribeiro [19] used the hierarchical finite element method to study nonlinear beam vibration, and thermal effects were considered by Manoach and Ribeiro [20], Librescu and co-workers [21], and Ribeiro and Monach [22]. Additional formulations have been given by Cottrell and co-workers [23] and Cao and Tucker [24]. More recent studies of nonlinear beam vibration have incorporated nonlocal elasticity or a modified couple stress or strain gradient theory [25–28]. Other studies have considered beams on elastic foundations [29], functionally graded beams [30], collocation methods [31], and high order strain gradient theories [32]. Additional models using a unified beam theory have been presented by Pagana and Carrera [33] and applied to rotating beams by Fillippi, Pagana, and Carrera [34].

The axial vibration of the beam continuum has not seen near the attention of flexural vibrations, at least in the nonlinear geometric realm. Some studies have included one-dimensional models in which the restoring force is assumed to be of third-order [35], and others have studied axial vibrations that contain the strain components that are quadratic in the axial displacement gradient in modeling nanotubes [36] and nonlinear elastic properties of cow muscle [37]. Both continuous and discretized axial bar vibrations that contain exactly cubic nonlinearities have also been studied [38,39]. But studies of the influence of geometric nonlinearity on the frequency of axial vibration are relatively unknown.

In this study, the large-amplitude nonlinear vibration behavior is studied for both the axial (or longitudinal) and flexural (or bending) modes of isotropic and anisotropic beams using both the one-dimensional Euler–Bernoulli beam as a representative example of simplified theories and a more comprehensive total Lagrangian description of the planar solid that comprises the beam. Both formulations are

* Corresponding author.
E-mail address: prh@engr.colostate.edu (P.R. Heyliger).

https://doi.org/10.1016/j.ijnonlinmec.2019.103286
Received 22 March 2019; Received in revised form 20 September 2019; Accepted 23 September 2019
Available online 25 September 2019

developed, discussed, and applied to several geometries that have been considered in past work to determine the level of influence of several of the kinematic variables that can influence the increase in nonlinear frequency compared with linear values. The total Lagrangian formulation does not reduce or approximate the nonlinear strain terms as is the case in many other studies and so provides a more complete analysis of the system. The frequencies can be found using direct iteration with the updated eigenfunction approximations provided that an appropriate number of terms are used to represent the two in-plane displacements.

2. Theory

In this section, the problem geometry and character are defined and the two primary methods of analysis are outlined.

2.1. Geometry

The geometry considered in this study is a prismatic rectangular beam with a length of L, a height of H, and a width of b. For all models considered in this study, the out-of-plane displacement is assumed to be zero as all motion is confined to an $x-z$ plane. The material response is assumed to follow a linear constitutive law and is characterized by the elastic modulus E and the Poisson ratio ν for isotropic materials. For anisotropic beams, the material properties are represented by the four inplane engineering constants E_1, E_2, ν_{12}, and G_{12}, where the first two values are the elastic modulii in the two principal material directions, the third is the in-plane Poisson ratio, and the final is the in-plane shear modulus. The boundary conditions at the left and right ends of the beam are discussed for specific examples to follow, but the upper and lower surfaces of the beam are assumed to be traction-free. The material has a density of ρ.

For the bulk of the work in this study, the domain is two-dimensional with the origin of an (x, z) system located at the beam centroid at the left-hand end of the beam. For the Euler–Bernoulli beam model, the thickness coordinate z is pre-integrated out of the governing differential equations and lumped into equivalent cross-sectional properties including the area A and the second moment of the area I. For the total Lagrangian plane elasticity model, these resultants are not used.

2.2. One dimensional models

By far, most early studies of nonlinear beam response have used the kinematic model implied by Euler–Bernoulli beam theory coupled with axial bar mechanics. In this case, the governing equations of motion can be given as [40]

$$\frac{\partial}{\partial x}\left\{AE\left[\frac{\partial u}{\partial x}+\frac{1}{2}\left(\frac{\partial w}{\partial x}\right)^2\right]\right\}+f=\rho A\frac{\partial^2 u}{\partial t^2} \tag{1}$$

$$-\frac{\partial^2}{\partial x^2}\left(EI\frac{\partial^2 w}{\partial x^2}\right)+\frac{\partial}{\partial x}\left\{AE\frac{\partial w}{\partial x}\left[\frac{\partial u}{\partial x}+\frac{1}{2}\left(\frac{\partial w}{\partial x}\right)^2\right]\right\}+q=\rho A\frac{\partial^2 w}{\partial t^2} \tag{2}$$

Here x is the independent spatial coordinate along the length of the beam, t is time, E is the modulus of elasticity in the axial direction of the beam, u and w are the axial and transverse displacements of the section centroid, A is the area of the cross-section, ρ is the material density, and f and q are the distributed axial and transverse loads, respectively. For the free vibration problem, these last two variables are assumed to be zero. This one-dimensional model embeds several key assumptions, the most prominent of which are (1) the constraint of zero shear strain in the kinematic model, which is cause for concern as the slenderness ratio of the beam decreases, (2) ignoring rotary inertia, which is also an issue as the beam becomes thick, and (3) the neglect of any material anisotropy. All of these are discussed within the context of the present planar elasticity model.

The term that couples the axial and transverse motion for the one-dimensional theory is the rotation $(\partial w/\partial x)$ that appears in both equations. When this value is small in the case of small displacements and rotations, the two equations uncouple and they represent motion in the axial and transverse directions, respectively. The solutions to both of these problems under free vibration conditions are well-known [41]. As the rotation increases in size, the coupling becomes more pronounced as the axial force increases with the amplitude of transverse motion and cannot be ignored.

The finite element model of this system has been given by Reddy [40] for the static case but can be easily adjusted to include the kinetic terms in the equations of motion and assumption of simple harmonic motion in the axial and transverse displacement variables. This results in the generalized eigenvalue problem

$$\begin{bmatrix}[K_{11}] & [K_{12}]\\ [K_{21}] & [K_{22}]\end{bmatrix}\begin{Bmatrix}\{u\}\\ \{\Delta\}\end{Bmatrix}=\omega^2\begin{bmatrix}[M_{11}] & [0]\\ [0] & [M_{22}]\end{bmatrix}\begin{Bmatrix}\{u\}\\ \{\Delta\}\end{Bmatrix} \tag{3}$$

Here the finite element variables of displacement and rotation have been embedded within the vector Δ as is common for this sort of structural system. Both the element matrices and the global matrix have the exact same structure. The elements within the submatrices are defined in the Appendix in closed form in terms of nodal variables. For linear analysis, the off-diagonal matrices are zero and there is no interaction between the axial and transverse displacements. Hence the analysis results in uncoupled axial and bending vibrational modes which can be solved for the natural frequencies ω along with the resulting eigenvectors u and Δ for the axial and bending vibrational modes. In nonlinear analysis, direct iteration can be used to constantly update the matrices on the left-hand side by normalizing the eigenvector according to the maximum displacement in the beam. This allows a scaling of the nonlinear terms that can be updated within the global $[K]$ matrix. This equation is solved iteratively for the unknown frequency ω until convergence has been achieved. In this study, convergence is assumed when the frequency does not change in the fifth decimal point between iterations.

The boundary conditions for this model are simple to enforce. For pinned conditions, the axial displacement and the transverse displacement are set equal to zero. For clamped conditions, the beam rotation $(\partial w/\partial x)$ is also set equal to zero in addition to the two displacements. All of these values are measured at the beam centroid since the beam displacement field has already incorporated the thickness coordinate into the Euler–Bernoulli kinematic assumptions. This finite element model was used as a means of comparison for all flexural mode results that follow.

2.3. Total Lagrangian plane elasticity model

Several excellent descriptions of the large deformation behavior of solids are available [42,43]. In this section only the elements that are of critical importance to the vibrating beam problem using elasticity theory rather than simplified beam models are highlighted.

The starting point for the analysis using nonlinear plane elasticity theory is a dynamic form of spatial virtual work, which can be expressed as

$$\int_V \sigma_{ij}\delta d_{ij}dV-\int_V f_i\delta v_i dV-\int_S t_i\delta v_i dS=\int_V \rho\frac{\partial^2 u_i}{\partial t^2}\delta v_i dV \tag{4}$$

Here V and S are the volume and surface occupied by and bounding the solid in the deformed configuration, t_i and f_i are the components of the specified surface tractions and body force vectors, δ is the variational operator, σ_{ij} are the components of the Cauchy stress tensor, d_{ij} is the rate of deformation tensor, and u_i and v_i are the components of displacement and velocity.

Under the type of free vibration motion such as that considered in this study, the displacements are assumed to have a sinusoidal dependence in time and the body force and surface tractions are equal to zero. This latter condition eliminates the second and third integrals

on the left hand side. In addition, it can be shown that in a total Lagrangian description the double product of the Cauchy stress and its energetic work conjugate of the rate of deformation tensor integrated over the deformed volume is the same as the integral over the original volume ${}^0V$. Hence

$$\int_V \sigma_{ij}\delta d_{ij} dV = \int_{{}^0V} {}^2_0S_{ij}\delta {}^2_0\dot{E}_{ij} d^0V \tag{5}$$

Here ${}^2_0S_{ij}$ are the components of the second Piola–Kirchhoff stress tensor in the deformed configuration referred to the initial configuration ${}^0V$ and ${}^2_0\dot{E}_{ij}$ are the components of the material strain rate tensor. In the case of harmonic motion, which is the nature of the deformation in the course of this study, the time derivatives of the displacements all contain a common term that cancels. Hence the equivalent quasi-static forms can be used where

$$\int_V \sigma_{ij}\delta\epsilon_{ij} dV = \int_{{}^0V} {}^2_0S_{ij}\delta {}^2_0E_{ij} d^0V \tag{6}$$

Here ϵ_{ij} and ${}^2_0E_{ij}$ are the components of the Cauchy infinitesimal strain and the Green–Lagrange strain tensors, respectively. The constitutive model for the second Piola–Kirchhoff stress is assumed to be written in the form

$${}^2_0S_{ij} = {}_0C_{ijkl}\,{}^2_0E_{ij} \tag{7}$$

Here ${}_0C_{ijkl}$ are the components of the elastic stiffness tensor in the original configuration of the beam. The components of Green–Lagrange strain can be expressed in terms of the total displacement components ${}^2_0u_i$ measured from the undeformed configuration (0) to the deformed configuration (2) in the three coordinate directions x_i as

$${}^2_0E_{ij} = \frac{1}{2}\left(\frac{\partial^2_0 u_i}{\partial^0 x_j} + \frac{\partial^2_0 u_j}{\partial^0 x_i} + \frac{\partial^2_0 u_m}{\partial^0 x_i}\frac{\partial^2_0 u_m}{\partial^0 x_j}\right) \tag{8}$$

Substituting these expressions into the remaining terms, dropping the left superscript and subscripts on the displacements for convenience by letting ${}^2_0u_1 = u$, ${}^2_0u_3 = w$, $x_1 = x$, and $x_3 = z$, and using the prior assumption of harmonic motion (where, for example, $u(x,z,t) = u(x,z)\sin\omega t$ where ω is the natural frequency of free vibration, results in the weak form of the equations of harmonic motion given by

$$\begin{aligned}
&\int_{{}^0V}\Bigg\{ C_{11}\left[\frac{\partial u}{\partial x} + \frac{1}{2}\left(\frac{\partial u}{\partial x}\right)^2 + \frac{1}{2}\left(\frac{\partial w}{\partial x}\right)^2\right] \\
&\quad + C_{13}\left[\frac{\partial w}{\partial z} + \frac{1}{2}\left(\frac{\partial u}{\partial z}\right)^2 + \frac{1}{2}\left(\frac{\partial w}{\partial z}\right)^2\right]\Bigg\} \\
&\quad \left[\frac{\partial \delta u}{\partial x} + \left(\frac{\partial u}{\partial x}\right)\left(\frac{\partial \delta u}{\partial x}\right) + \left(\frac{\partial w}{\partial x}\right)\left(\frac{\partial \delta w}{\partial x}\right)\right] + \\
&\quad \Bigg\{ C_{13}\left[\frac{\partial u}{\partial x} + \frac{1}{2}\left(\frac{\partial u}{\partial x}\right)^2 + \frac{1}{2}\left(\frac{\partial w}{\partial x}\right)^2\right] \\
&\quad + C_{33}\left[\frac{\partial w}{\partial z} + \frac{1}{2}\left(\frac{\partial u}{\partial z}\right)^2 + \frac{1}{2}\left(\frac{\partial w}{\partial z}\right)^2\right]\Bigg\} \\
&\quad \left[\frac{\partial \delta w}{\partial z} + \left(\frac{\partial u}{\partial z}\right)\left(\frac{\partial \delta u}{\partial z}\right) + \left(\frac{\partial w}{\partial z}\right)\left(\frac{\partial \delta w}{\partial z}\right)\right] + \\
&\quad C_{55}\left[\left(\frac{\partial u}{\partial z} + \frac{\partial w}{\partial x}\right) + \frac{\partial u}{\partial x}\frac{\partial u}{\partial z} + \frac{\partial w}{\partial x}\frac{\partial w}{\partial z}\right] \\
&\quad \left[\left(\frac{\partial \delta u}{\partial z} + \frac{\partial \delta w}{\partial x}\right) + \frac{\partial \delta u}{\partial x}\frac{\partial u}{\partial z} + \frac{\partial u}{\partial x}\frac{\partial \delta u}{\partial z} + \frac{\partial \delta w}{\partial x}\frac{\partial w}{\partial z} + \frac{\partial w}{\partial x}\frac{\partial \delta w}{\partial z}\right] dV \\
&\quad = \omega^2 \int_{{}^0V} \rho_0(u\delta u + w\delta w) dV
\end{aligned} \tag{9}$$

In this study, Ritz-based approximations are sought for the two in-plane displacement components u and w and their variations in the form

$$u(x,z) = \sum_{j=1}^{M} a_j \psi^u_j(x,z) \qquad \delta u = \psi^u_i(x,z) \tag{10}$$

$$w(x,z) = \sum_{j=1}^{N} b_j \psi^w_j(x,z) \qquad \delta w = \psi^w_i(x,z) \tag{11}$$

Here M and N are the total number of approximations used for the displacements in the x and z directions, respectively. Substituting these into the weak form allows expression of the final generalized eigenvalue problem to be written in matrix form as

$$\begin{bmatrix} [K^1_{11} + K^2_{11}] & [K^1_{13} + K^2_{13}] \\ [K^1_{31} + K^2_{31}] & [K^1_{33} + K^2_{33}] \end{bmatrix} \begin{Bmatrix} \{a\} \\ \{b\} \end{Bmatrix} = \omega^2 \begin{bmatrix} [M_{uu}] & [0] \\ [0] & [M_{ww}] \end{bmatrix} \begin{Bmatrix} \{a\} \\ \{b\} \end{Bmatrix} \tag{12}$$

Here the superscripts of 1 and 2 represent contributions from the linear and nonlinear terms in the weak statement, respectively. As before, the linear versions of these equations are initially solved to obtain the initial eigenvalues for the Ritz constants. The displacements and their gradients are then computed over the entire domain using these displacement functions scaled to some fixed amplitude a at a single location in the beam and used in the nonlinear coefficient matrices as updates. The process then repeats until there is no change in the fifth decimal place of the nonlinear frequencies from one iteration to the next.

3. Applications

Several representative cases were considered for the dominant modes of deformation for the representative geometry under longitudinal and flexural vibrations. It is not typical to use the phrase *beam* in the context of longitudinal vibrations, but because of the nonlinear coupling it is used in the results that follow and the words *bar* and *beam* are effectively interchangeable.

3.1. Longitudinal vibrations

There is a special case embedded within the kinematic models assumed here using elasticity theory. This is the case where the mode of vibration is not associated with flexure or shear but rather the longitudinal deformation along the axis of the beam. Such modes are purely axial and linear according to the one-dimensional theories since in this case the transverse displacement of the beam centroid is exactly zero. For the elasticity model, there are nonlinear terms associated with the squares or products of the displacement gradients along with non-zero transverse normal strains that are usually neglected in one-dimensional theories and have seen little if any exploration in existing studies of bar and beam dynamics.

There is another behavior that influences frequency response for both linear and nonlinear analysis, and that is the Poisson effect in the region of supports. In one-dimensional models, these effects are almost always neglected. Yet there is a stiffening effect that can occur in such regions, and this changes the nature of the displacement field in the region of, for example, fixed supports.

To investigate these effects, a fixed-fixed rectangular bar is assumed to be under the constraint of plane stress. The classical linear one-dimensional bar theory predicts frequencies of a bar of length L with elastic modulus E and density ρ to be given by [41]

$$\omega_n = \frac{n\pi}{L}\sqrt{\frac{E}{\rho}} \tag{13}$$

These frequencies are of course independent of the Poisson ratio and there is no impact of the support restraint on the transverse displacement since those values are assumed be zero.

This problem is considered using the plane elasticity methodology using approximation functions for both displacement components to be of the form

$$\psi^u_i(x,z) = \psi^w_j(x,z) = \sin\frac{j\pi x}{L} z^{k-1} \tag{14}$$

Here the indices i, j, and k are independent and range outside of the values 1, 2, 3 usually used with indicial notation. The origin of the (x,z) system is at the left end centroid. The index i is simply a counter for the number of independent approximations formed by the products of the spatial approximations in x (identified by the index j) and

the power series approximations in the thickness coordinate z, which are identified by the index k. This family of approximation functions contains the one-dimensional eigenfunctions for the fixed-fixed axial bar for the linear solution of free vibration.

3.2. Flexural vibrations

Of primary interest in the nonlinear range are cases where there is some sort of restraint that results in an axial force generated along the beam length during flexural vibration. This has the effect of stiffening the beam and the nonlinear frequencies are larger than those developed for pure bending without this axial coupling. In the present formulation, the nonlinear aspects of the problem are directly considered by including the nonlinear terms in the Green–Lagrange strain tensor as they appear in the original statement of virtual work. The dominant nonlinear term is the square of the transverse displacement gradient $\partial w/\partial x$ that appears in the one-dimensional theory. This is the so-called Föppl–von Karman nonlinearity [44,45]. In the full planar elasticity formulation, however, there are far more terms that can appear just as for the case of nonlinear axial vibration as noted in the form of the element equations in Appendix.

3.2.1. Clamped–clamped support

In this case the approximation functions are exactly the same as those used for the case of the fixed-fixed bar under axial vibration. However, the focus is now on the eigenvectors associated with the lowest bending mode rather than the lowest axial mode. Only odd and even functions were used for the bending and axial displacement functions, respectively, to capture the lowest bending mode behavior.

3.2.2. Simple support

The case of simple support using elasticity theory requires a bit more care than the case of clamped–clamped conditions. In general, the transverse displacement should be zero at both ends of the beam and the axial displacement should be non-zero at the ends and change sign both in z and at the two support locations. Hence in general the approximations used are of the form

$$\psi_i^u(x,z) = \cos\frac{j\pi x}{L} z^{2k-1} \tag{15}$$

$$\psi_i^w(x,z) = \sin\frac{j\pi x}{L} z^{k-1} \tag{16}$$

However, this type of function does not allow an axial force to develop along the length of the beam. The axial displacements must be supplemented with approximating functions of the form

$$\psi_i^u(x,z) = \sin\frac{2i\pi x}{L} \tag{17}$$

These additional functions are necessary because they are the only conditions that can generate a non-zero axial force that does not vary with beam thickness. The resultant forces generated from the axial displacement associated with bending are equal to zero because of the odd nature of the initial axial displacement functions in the thickness coordinate. The factor of 2 within the sine function assumes that the primary mode is the initial flexural mode, in which the axial displacements are antisymmetric about the mid-point of the beam.

In all the results that follow, functions up to seventh order both along the axis and through the thickness are used to describe all displacement functions. For the inplane axial supplemental terms, a total of three functions are included. These functions were selected after representative convergence studies on both the axial and transverse vibrational modes. Hence if only odd functions are included in both x and z, this implies that M = 19 and N = 16 in Eqs. (10) and (11).

For isotropic materials, a value of Poisson ratio of either zero or 0.3 was used for the examples that follow. The elastic modulus and the material density are somewhat arbitrary since results are given as a function of frequency ratios and hence these values cancel. For the orthotropic material, the properties of a graphite-polymer composite were used as typical of the large mismatch between the longitudinal and in-plane shear modulus that can occur in many materials. The engineering properties are given as E_1 = 155.0 GPa, $E_2 = E_3$ = 12.10 GPa, ν_{23} = 0.458, $\nu_{12} = \nu_{13}$ = 0.248, G_{23} = 3.20 GPa, and $G_{13} = G_{12}$ = 4.40 GPa [46]. In all cases, the lowest mode of the type of vibration was used for the iterated eigenvalue in the nonlinear analysis.

Table 1
Ratio of $(\omega_{NL}/\omega_L)^2$ for the hinged–hinged isotropic beam and compared with the higher-order and Euler–Bernoulli beam theory results.

a/r	L/r = 13.856		L/r = 27.713		L/r = 110.85		Euler–Bernoulli	
	[13]	Present	[13]	Present	[13]	Present	[2]	1DFEM
0.1	1.0028	1.0032	1.0026	1.0028	1.0025	1.0026	1.0025	1.0025
0.2	1.0112	1.0128	1.0102	1.0111	1.0099	1.0105	1.0100	1.0100
0.4	1.0449	1.0514	1.0409	1.0443	1.0396	1.0421	1.0400	1.0400
0.6	1.1010	1.1159	1.0921	1.0997	1.0891	1.0947	1.0900	1.0900
0.8	1.1792	1.2066	1.1635	1.1774	1.1584	1.1684	1.1600	1.1598
1.0	1.2795	1.3239	1.2554	1.2773	1.2474	1.2632	1.2500	1.2496
1.5	1.6247	1.7378	1.5736	1.6258	1.5566	1.5921	1.5625	1.5605
2.0	2.1003	2.3331	2.0171	2.1224	1.9886	2.0527	2.0000	1.9939

Table 2
Ratio of $(\omega_{NL}/\omega_L)^2$ for the clamped–clamped isotropic beam and compared with the higher-order and Euler–Bernoulli beam theory results.

a/r	L/r = 13.856		L/r = 27.713		L/r = 110.85		Euler–Bernoulli	
	[13]	Present	[13]	Present	[13]	Present	1DFEM	[6]
0.1	1.0009	1.0009	1.0007	1.0007	1.0006	1.0006	1.0006	1.0006
0.2	1.0036	1.0036	1.0027	1.0029	1.0024	1.0024	1.0025	1.0024
0.4	1.0146	1.0143	1.0107	1.0115	1.0096	1.0097	1.0096	1.0096
0.6	1.0328	1.0321	1.0240	1.0257	1.0217	1.0219	1.0215	1.0216
0.8	1.0582	1.0570	1.0428	1.0457	1.0385	1.0389	1.0382	1.0384
1.0	1.0911	1.0891	1.0668	1.0714	1.0602	1.0607	1.0597	1.0599
1.5	1.2039	1.2004	1.1496	1.1603	1.1352	1.1361	1.1339	1.1349
2.0	1.3594	1.3561	1.2643	1.2839	1.2397	1.2410	1.2371	1.2398

Table 3
Ratio of $(\omega_{NL}/\omega_L)^2$ for the hinged–hinged and clamped–clamped anisotropic beams.

a/r	Hinged–hinged			Clamped–clamped		
	L/r			L/r		
	13.856	27.713	110.85	13.856	27.713	110.85
0.1	1.0077	1.0039	1.0026	1.0052	1.0017	1.0008
0.2	1.0307	1.0155	1.0104	1.0207	1.0068	1.0034
0.4	1.1232	1.0619	1.0417	1.0829	1.0273	1.0136
0.6	1.2782	1.1393	1.0938	1.1873	1.0613	1.0305
0.8	1.4962	1.2479	1.1668	1.3347	1.1091	1.0542
1.0	1.7781	1.3878	1.2606	1.5262	1.1705	1.0845
1.5	2.7744	1.8755	1.5863	2.2031	1.3843	1.1894
2.0		2.5623	2.0432		1.6862	1.3348

4. Results

For the nonlinear axial frequency, the squared frequency ratio as a function of a/r is shown in Fig. 1 for the case of the isotropic bar where a is the peak amplitude within the bar and r is the radius of gyration $\sqrt{I/A}$. The mode shapes for the axial bar are shown for three different cases in Fig. 2: the isotropic bar with an assumed zero Poisson ratio, the isotropic bar with full elastic properties, and the anisotropic bar with the stiff (1) direction along the bar axis.

The squared frequency ratios for the isotropic hinged–hinged beam for the present model are compared with the results from the higher-order beam theory [13], the analytic Euler–Bernoulli model [2], and the one-dimensional Euler–Bernoulli finite element model developed in this work in Table 1 both as a function of the slenderness ratio L/r and the relative amplitude of vibration a/r. A similar comparison is given for the clamped–clamped beam in Table 2. The results for the anisotropic beam are shown in Table 3 for both the hinged–hinged and

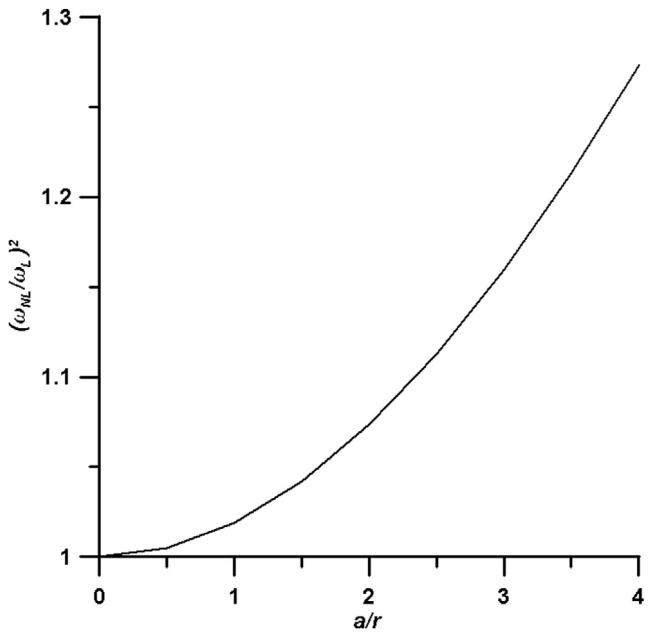

Fig. 1. The ratio of squared frequency as a function of aspect ratio for the clamped–clamped axial bar under its fundamental vibrational mode.

the clamped–clamped beam. Since the Euler–Bernoulli results depend only on the value of the elastic modulus in the axial direction of the beam, the frequency ratios for the anisotropic case can be compared with the analytic or finite element results that are given for the isotropic beams in Tables 1 and 2. As a check on the present method, analyses were repeated using the kinematic model of the Euler–Bernoulli beam with the Föppl–von Karman nonlinearity. These results were identical to those of the comparative studies presented here.

Representative modal plots of the lowest nonlinear frequency are given in Fig. 3 for the isotropic and anisotropic beam. The one-dimensional results are plotted along the beam centerline from the finite element results developed in this work since the position of the centroidal axis completely defines the state of deformation for the Euler–Bernoulli beam.

5. Discussion

There are few, if any, results with which to compare the axial frequencies. Although only the case of the isotropic material with a non-zero Poisson ratio is shown, the results in Fig. 1 are nearly identical to those when the Poisson ratio is zero and also for the anisotropic bar. Likewise, there is little to no change as a function of the aspect ratio for the axial modes results. More interesting are the modal plots for the axial modes shown in Fig. 2. The transverse displacement varies widely as a function of the Poisson effect, and the displacements for the anisotropic bar are especially pronounced because of the large mismatch between the elastic modulii E_1 and E_2.

There is very good agreement between the present elasticity model and the results from the higher-order beam theory for the flexural isotropic modes. However, the frequencies for the former model are consistently higher than those of the latter for all but the short thick beam under clamped conditions.

For the anisotropic beam, the increase in frequency ratio is far larger than for that of the isotropic beam. For example, the squared frequency ratio for the aspect ratio of 13.856 with $a/r = 1$ is 1.7378 for the for isotropic beam but 2.7744 for the anisotropic beam. Much of this difference is because of the larger levels of shear deformation for the anisotropic beam. This is very clearly demonstrated in the modal plots of Fig. 3. There is significant shear deformation in the isotropic case but it is not as obvious as the clear deviation in the straight-line normals to the centroidal axis for the anisotropic beam.

6. Conclusions

The analysis based in this study is based on an elasticity formulation that does not restrict or eliminate any of the terms in the expression for nonlinear strain. Based on the results of this work, preliminary conclusions can be listed as follows:

1. Initial estimates of nonlinear frequency response indicates several percent increase over linear values for $a/r = 1$ and a ten percent difference for $a/r = 2.25$.

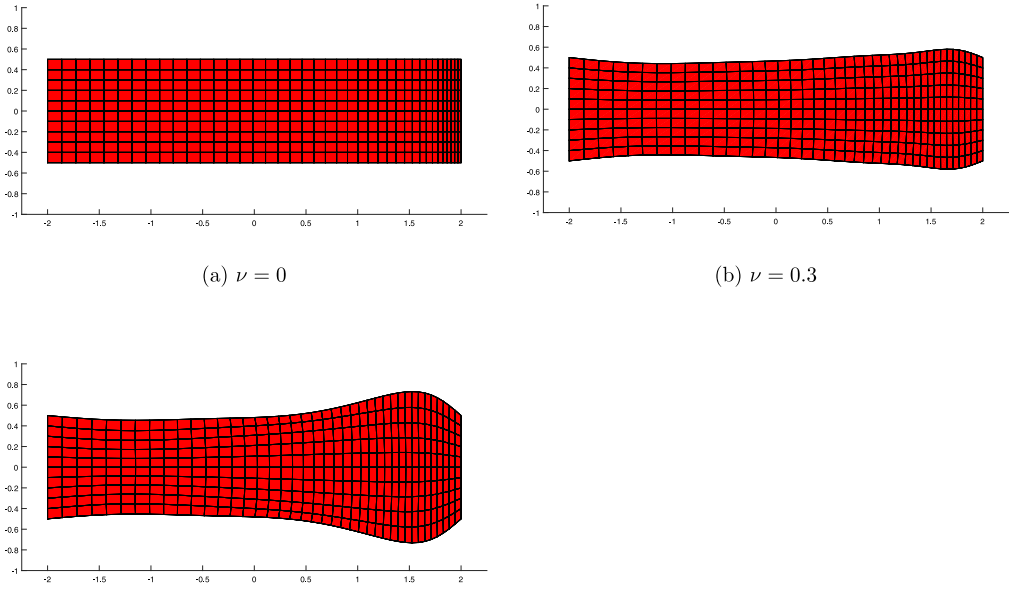

(a) $\nu = 0$ (b) $\nu = 0.3$

(c) Anisotropic

Fig. 2. The lowest nonlinear axial mode for the fixed-fixed bar of length $L/H = 4$ with $a/r = 2$, plotted to scale with and without Poisson effects at the supports.

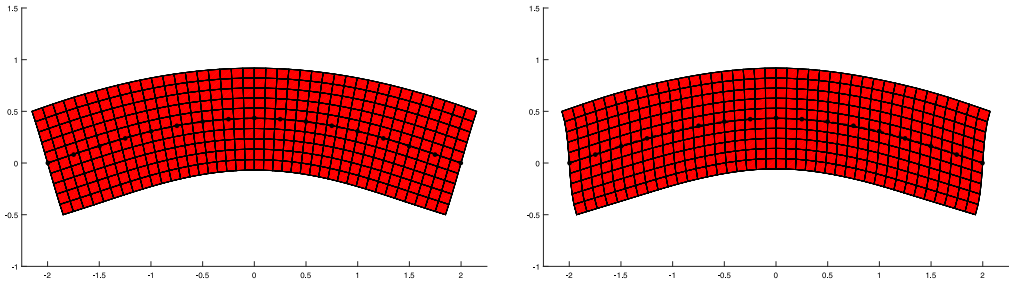

(a) Isotropic beam (b) Anisotropic beam

Fig. 3. The lowest bending mode for the simply supported beam with $L/H = 4$ and $a/r = 1.5$, plotted to scale for the isotropic and anisotropic case.

2. A full nonlinear planar elasticity model gives a ratio of the square of nonlinear to linear frequency ratios that are greater than those of the higher order beam theory by up to ten percent for a/r of 2, and greater than the Euler–Bernoulli frequency ratios by over 15 percent for thicker isotropic beams.
3. For isotropic beams, moderately large amplitude vibrations of up to $a/r = 1$ for slenderness ratios up to about 25 are modeled within several percent of plane elasticity models by nonlinear one-dimensional Euler–Bernoulli beam theory. For higher values of a/r and L/r, the higher order theory gives results that are in excellent agreement with those from plane elasticity.
4. For the representative case of anisotropic media, where the shear modulus and off-direction elastic modulus are at least one order of magnitude smaller than the on-direction modulus, Euler–Bernoulli theory is completely inadequate even for relatively slender beams. Even the higher order beam model gives frequency ratios that appear to under-predict those from the present formulation. The combination of shear deformation and the contribution of nonlinear terms other than that of Föppl–von Karman yield squared frequency ratios with far larger differences as the beam becomes thick. It appears that existing models for nonlinear beam vibration fall short when the material is anisotropic, and improved simplified beam theories await development.

Declaration of competing interest

The authors declare that they have no known competing financial interests or personal relationships that could have appeared to influence the work reported in this paper.

Appendix

The element matrices for the one-dimensional nonlinear Euler–Bernoulli beam model where the displacements depend only on the axial coordinate x can be expressed as

$$K_{ij}^{11} = \int_{x_A}^{x_B} AE \frac{d\psi_i}{dx}\frac{d\psi_j}{dx} dx \tag{18}$$

$$K_{ij}^{12} = \int_{x_A}^{x_B} \frac{1}{2} AE \frac{dw}{dx}\frac{d\psi_i}{dx}\frac{d\phi_j}{dx} dx \tag{19}$$

$$K_{ij}^{21} = \int_{x_A}^{x_B} AE \frac{dw}{dx}\frac{d\psi_i}{dx}\frac{d\phi_j}{dx} dx \tag{20}$$

$$K_{ij}^{22} = \int_{x_A}^{x_B} EI \frac{d^2\psi_i}{dx^2}\frac{d^2\phi_j}{dx^2} dx + \int_{x_A}^{x_B} \frac{1}{2} AE \left(\frac{dw}{dx}\right)^2 \frac{d\phi_i}{dx}\frac{d\phi_j}{dx} dx dx \tag{21}$$

The terms in K_{ij}^{11} and the terms in the first integral of K_{ij}^{22} are well-known when linear approximations are used for the axial displacements and Hermite cubic polynomials are used for the transverse displacements. The nonlinear terms are those that involve (dw/dx) and can be evaluated analytically. They are given in matrix form for an element of length h as

$$\begin{bmatrix} 0 & K_{11}^{12} & K_{12}^{12} & 0 & K_{12}^{13} & K_{12}^{14} \\ K_{11}^{21} & K_{11}^{22} & K_{12}^{22} & K_{12}^{21} & K_{13}^{22} & K_{14}^{22} \\ K_{21}^{21} & K_{12}^{22} & K_{22}^{22} & K_{12}^{21} & K_{23}^{22} & K_{24}^{22} \\ 0 & K_{21}^{12} & K_{22}^{12} & 0 & K_{23}^{12} & K_{24}^{12} \\ K_{31}^{21} & K_{13}^{22} & K_{23}^{22} & K_{41}^{21} & K_{33}^{22} & K_{34}^{22} \\ K_{41}^{21} & K_{14}^{22} & K_{24}^{22} & K_{42}^{21} & K_{34}^{22} & K_{44}^{22} \end{bmatrix} \tag{22}$$

$$K_{11}^{12} = \frac{AE}{20h^2}\left(-12\Delta_1 + h\Delta_2 + 12\Delta_3 + h\Delta_4\right) = \frac{1}{2}K_{11}^{21} = -K_{21}^{12} \tag{23}$$

$$K_{12}^{12} = \frac{AE}{60h}\left(3\Delta_1 - 4h\Delta_2 - 3\Delta_3 + h\Delta_4\right) = \frac{1}{2}K_{12}^{21} = -K_{22}^{12} \tag{24}$$

$$K_{13}^{12} = \frac{AE}{20h^2}\left(12\Delta_1 - h\Delta_2 - 12\Delta_3 - h\Delta_4\right) = \frac{1}{2}K_{31}^{21} = -K_{23}^{12} \tag{25}$$

$$K_{14}^{12} = \frac{AE}{60h}\left(3\Delta_1 + h\Delta_2 - 3\Delta_3 - 4h\Delta_4\right) = \frac{1}{2}K_{41}^{21} = -K_{24}^{12} \tag{26}$$

$$K_{11}^{22} = \frac{3AE}{70h^3}\left(6\Delta_3\Delta_4 h - 6\Delta_1\Delta_4 h + 6\Delta_2\Delta_3 h - 6\Delta_1\Delta_2 h + \Delta_2^2h^2 + 24\Delta_1^2 - 48\Delta_1\Delta_3 + 24\Delta_3^2 + \Delta_4^2h^2\right) \tag{27}$$

$$K_{12}^{22} = \frac{AE}{280h^2}\left(-2\Delta_2\Delta_4 h^2 - 24\Delta_2\Delta_3 h + 24\Delta_1\Delta_2 h + \Delta_2^2h^2 - 36\Delta_1^2 + 72\Delta_1\Delta_3 - 36\Delta_3^2 - \Delta_4^2h^2\right) \tag{28}$$

$$K_{13}^{22} = \frac{-3AE}{70h^3}\left(6\Delta_3\Delta_4 h - 6\Delta_1\Delta_4 h + 6\Delta_2\Delta_3 h - 6\Delta_1\Delta_2 h + 24\Delta_1^2 - 48\Delta_1\Delta_3 + 24\Delta_3^2 + \Delta_4^2h^2\right) \tag{29}$$

$$K_{14}^{22} = \frac{-AE}{280h^2}\left(24\Delta_3\Delta_4 h - 24\Delta_1\Delta_4 h + 2\Delta_2\Delta_4 h^2 + \Delta_2^2h^2 + 36\Delta_1^2 - 72\Delta_1\Delta_3 + 36\Delta_3^2 - \Delta_4^2h^2\right) \tag{30}$$

$$K_{22}^{22} = \frac{AE}{420h}\left(3\Delta_3\Delta_4 h - 3\Delta_1\Delta_4 h - 3\Delta_2\Delta_4 h^2 - 3\Delta_2\Delta_3 h + 12\Delta_2^2h^2 + 18\Delta_1^2 - 36\Delta_1\Delta_3 + 18\Delta_3^2 + \Delta_4^2\right) \tag{31}$$

$$K_{23}^{22} = \frac{-AE}{280h^2}\left(-2\Delta_2\Delta_4 h^2 - 24\Delta_2\Delta_3 h + 24\Delta_1\Delta_2 h + \Delta_2^2h^2 - 36\Delta_1^2 + 72\Delta_1\Delta_3 - 36\Delta_3^2 - \Delta_4^2h^2\right) \tag{32}$$

$$K_{24}^{22} = \frac{AE}{840}\left(6\Delta_3\Delta_4 - 6\Delta_1\Delta_4 + 4\Delta_2\Delta_4 h + 6\Delta_2\Delta_3 - 6\Delta_1\Delta_2 - 3\Delta_2^2 h - 3\Delta_4^2 h\right) \tag{33}$$

$$\begin{aligned} K_{33}^{22} &= \frac{3AE}{70h^3}\left(6\Delta_3\Delta_4 h - 6\Delta_1\Delta_4 h + 6\Delta_2\Delta_3 h - 6\Delta_1\Delta_2 h + \Delta_2^2 h^2\right. \\ &\left. +24\Delta_1^2 - 48\Delta_1\Delta_3 + 24\Delta_3^2 + \Delta_4^2 h^2\right) \end{aligned} \tag{34}$$

$$\begin{aligned} K_{34}^{22} &= \frac{AE}{280h^2}\left(24\Delta_3\Delta_4 h - 24\Delta_1\Delta_4 h + 2\Delta_2\Delta_4 h^2 + \Delta_2^2 h^2 + \right. \\ &\left. 36\Delta_1^2 - 72\Delta_1\Delta_3 + 36\Delta_3^2 - \Delta_4^2 h^2\right) \end{aligned} \tag{35}$$

$$\begin{aligned} K_{44}^{22} &= \frac{AE}{420h}\left(-3\Delta_3\Delta_4 h + 3\Delta_1\Delta_4 h - 3\Delta_2\Delta_4 h^2 + 3\Delta_1\Delta_2 h + \right. \\ &\left. \Delta_2^2 h^2 + 18\Delta_1^2 - 36\Delta_1\Delta_3 + 18\Delta_3^2 + 12\Delta_4^2 h^2\right) \end{aligned} \tag{36}$$

The element equations for the total Lagrangian plane elasticity model can be expressed as

$${}^1K_{ij}^{11} = \int_V \left(C_{11}\frac{\partial\psi_i^u}{\partial x}\frac{\partial\psi_j^u}{\partial x} + C_{55}\frac{\partial\psi_i^u}{\partial z}\frac{\partial\psi_j^u}{\partial z}\right) dV \tag{37}$$

$$\begin{aligned} {}^2K_{ij}^{11} &= \int_V \left[S_{11}\frac{\partial\psi_i^u}{\partial x}\frac{\partial\psi_j^u}{\partial x} + S_{33}\frac{\partial\psi_i^u}{\partial z}\frac{\partial\psi_j^u}{\partial z} + \right. \\ &S_{55}\left(\frac{\partial\psi_i^u}{\partial x}\frac{\partial\psi_j^u}{\partial z} + \frac{\partial\psi_i^u}{\partial z}\frac{\partial\psi_j^u}{\partial x}\right) + C_{11}\frac{\partial\psi_i^u}{\partial x}\frac{\partial\psi_j^u}{\partial x}\left(\frac{1}{2}\frac{\partial u}{\partial x}\right) \\ &\left. +C_{13}\frac{\partial\psi_i^u}{\partial x}\frac{\partial\psi_j^u}{\partial z}\left(\frac{1}{2}\frac{\partial u}{\partial z}\right)\right] dV \end{aligned} \tag{38}$$

$${}^1K_{ij}^{13} = \int_V \left(C_{13}\frac{\partial\psi_i^u}{\partial x}\frac{\partial\psi_j^w}{\partial z} + C_{55}\frac{\partial\psi_i^u}{\partial z}\frac{\partial\psi_j^w}{\partial x}\right) dV \tag{39}$$

$$\begin{aligned} {}^2K_{ij}^{13} &= \int_V \left[C_{11}\frac{\partial\psi_i^u}{\partial x}\frac{\partial\psi_j^w}{\partial x}\left(\frac{1}{2}\frac{\partial w}{\partial x}\right) + C_{13}\frac{\partial\psi_i^u}{\partial x}\frac{\partial\psi_j^w}{\partial z}\left(\frac{1}{2}\frac{\partial w}{\partial z}\right)\right. \\ &\left. +C_{55}\frac{\partial\psi_i^u}{\partial z}\frac{\partial\psi_j^w}{\partial z}\frac{\partial w}{\partial x}\right] dV \end{aligned} \tag{40}$$

$$\begin{aligned} {}^2K_{ij}^{31} &= \int_V \left[C_{13}\frac{\partial\psi_i^w}{\partial z}\frac{\partial\psi_j^u}{\partial x}\left(\frac{1}{2}\frac{\partial u}{\partial x}\right) + C_{33}\frac{\partial\psi_i^w}{\partial z}\frac{\partial\psi_j^u}{\partial z}\left(\frac{1}{2}\frac{\partial u}{\partial z}\right)\right. \\ &\left. +C_{55}\frac{\partial\psi_i^w}{\partial x}\frac{\partial\psi_j^u}{\partial x}\frac{\partial u}{\partial z}\right] dV \end{aligned} \tag{41}$$

$${}^1K_{ij}^{33} = \int_V \left(C_{33}\frac{\partial\psi_i^w}{\partial z}\frac{\partial\psi_j^w}{\partial z} + C_{55}\frac{\partial\psi_i^w}{\partial x}\frac{\partial\psi_j^w}{\partial x}\right) dV \tag{42}$$

$$\begin{aligned} {}^2K_{ij}^{33} &= \int_V \left[S_{11}\frac{\partial\psi_i^w}{\partial x}\frac{\partial\psi_j^w}{\partial x} + S_{33}\frac{\partial\psi_i^w}{\partial z}\frac{\partial\psi_j^w}{\partial z} + \right. \\ &S_{55}\left(\frac{\partial\psi_i^w}{\partial x}\frac{\partial\psi_j^w}{\partial z} + \frac{\partial\psi_i^w}{\partial z}\frac{\partial\psi_j^w}{\partial x}\right) + C_{13}\frac{\partial\psi_i^w}{\partial z}\frac{\partial\psi_j^w}{\partial x}\left(\frac{1}{2}\frac{\partial w}{\partial x}\right) \\ &\left. +C_{33}\frac{\partial\psi_i^w}{\partial z}\frac{\partial\psi_j^w}{\partial z}\left(\frac{1}{2}\frac{\partial w}{\partial z}\right)\right] dV \end{aligned} \tag{43}$$

References

[1] S.M. Han, H. Benaroya, T. Wei, Dynamics of transversely vibrating beams using four engineering theories, J. Sound Vib. 225 (1999) 935–988.

[2] S. Woinowsky-Krieger, The effect of an axial force on the vibration of hinged bars, J. Appl. Mech. 17 (1950) 35–36.

[3] D. Burgreen, Free vibrations of a pin-ended column with constant distance between end pins, J. Appl. Mech. 18 (1951) 135–139.

[4] J.D. Ray, C.W. Bert, Nonlinear vibrations of a beam with pinned ends, J. Eng. Ind. 91 (1961) 977–1004.

[5] A.V. Srinivasan, Large amplitude free oscillations of beams and plates, AIAA J. 3 (1965) 1951–1953.

[6] D.A. Evenson, Nonlinear vibrations of beams with various boundary conditions, AIAA J. 6 (1968) 370–372.

[7] G. Prathap, T.K. Varadan, The large amplitude vibration of hinged beams, Comput. Struct. 9 (1978) 219–222.

[8] G.R. Bhashyam, G. Prathap, Galerkin finite element method for nonlinear beam vibrations, J. Sound Vib. 72 (1980) 191–203.

[9] J.R. Reddy, I.R. Singh, Large deflections and large-amplitude free vibrations of straight and curved beams, Internat. J. Numer. Methods Engrg. 20 (1981) 829–852.

[10] B.S. Sarma, T.K. Varadan, Lagrange-Type formulation for finite element analysis of nonlinear beam vibrations, J. Sound Vib. (1983) 61–70.

[11] B.S. Sarma, T.K. Varadan, Ritz finite element approach to nonlinear vibrations of beams, Internat. J. Numer. Methods Engrg. 20 (1984) 353–387.

[12] B.S. Sarma, T.K. Varadan, Ritz finite element approach to nonlinear vibration of a timoshenko beam, Commun. Appl. Numer. Methods 1 (1985) 23–32.

[13] P.R. Heyliger, J.N. Reddy, A higher order beam finite element for bending and vibration problems, J. Sound Vib. 126 (1988) 309–326.

[14] P.F. Pai, A.H. Nayfeh, A fully nonlinear-theory of curved and twisted composite rotor blades accounting for warpings and 3-dimensional stress effects, Int. J. Sol. Struct. 31 (1994) 1309–1340.

[15] J. Mayo, J. Dominguez, A.A. Shabana, Geometrically nonlinear formulations of beams in flexible multibody dynamics, ASME J. Vib. Acoust. 117 (1995) 501–509.

[16] D.H. Hodges, X.Y. Shang, C.E.S. Cesnik, Finite element solution of nonlinear intrinsic equations for curved composite beams, J. Amer. Hel. Soc. 41 (1996) 313–321.

[17] R. Lewandowski, Computational formulation for periodic vibration of geometrically nonlinear structures, 2. numerical strategy and examples, Int. J. Sol. Struct. 34 (1997) 1949–1964.

[18] P. Ribeiro, M. Petyt, Non-linear vibration of beams with internal resonance by the hierarchical finite-element method, J. Sound Vib. 224 (1999) 591–624.

[19] P. Ribeiro, Hierarchical finite element analyses of geometrically non-linear vibration of beams and plane frames j, Sound Vib. 246 (2001) 225–244.

[20] E. Manoach, P. Ribeiro, Coupled, thermoelastic, Large amplitude vibrations of timoshenko beams, Int. J. Mech. Sci. 46 (2004) 1589–1606.

[21] L. Librescu, S.Y. Oh, O. S.O.ng, Thin-walled beams made of functionally graded materials and operating in a high temperature environment: Vibration and stability, J. Therm. Stresses 28 (2005) 649–712.

[22] P. Ribeiro, E. Manoach, The effect of temperature on the large amplitude vibrations of curved beams, J. Sound Vib. 285 (2005) 1093–1107.

[23] J.A. Cottrell, A. Reali, Y. Bazilevs, T.J.R. Hughes, Isogeometric analysis of structural vibrations, Comput. Methods Appl. Mech. Engrg. 195 (2006) 5257–5296.

[24] D.Q. Cao, R.W. Tucker, Nonlinear dynamics of elastic rods using the cosserat theory: Modelling and simulation, Int. J. Sol. Struct. 45 (2008) 460–477.

[25] J.N. Reddy, Microstructure-dependent couple stress theories of functionally graded beams, J. Mech. Phys. Sol. 59 (2011) 2382–2399.

[26] M. Asghari, M.H. Kahrobaiyan, M. Nikfar, M.T. Ahmadian, A size-dependent nonlinear timoshenko microbeam model based on the strain gradient theory, Acta Mech. 223 (2012) 1233–1249.

[27] M.H. Ghayesh, M. Amabili, H. Farokhi, Nonlinear forced vibrations of a microbeam based on the strain gradient elasticity theory, Internat. J. Engrg. Sci. 63 (2013) 52–60.

[28] H. Farokhi, M.H. Ghayesh, M. Amabili, Nonlinear dynamics of a geometrically imperfect microbeam based on the modified couple stress theory, Internat. J. Engrg. Sci. 68 (2013) 11–23.

[29] H. Yaghoobi, M. Torabi, Post-buckling and nonlinear free vibration analysis of geometrically imperfect functionally graded beams resting on nonlinear elastic foundation, Appl. Math. Mod. 37 (2013) 8324–8340.

[30] R. Ansari, T. Pourashraf, R. Gholami, An exact solution for the nonlinear forced vibration of functionally graded nanobeams in thermal environment based on surface elasticity theory, Thin-Walled Struct. 93 (2015) 169–176.

[31] A. Reali, H. Gomez, An isogeometric collocation approach for Bernoulli–euler beams and kirchhoff plates, Comput. Methods Appl. Mech. Engrg. 284 (2015) 623–636.

[32] S.M.H. Karparvarfard, M. Asghari, R. Vatankhah, A geometrically nonlinear beam model based on the second strain gradient theory, Internat. J. Engrg. Sci. 91 (2015) 63–75.

[33] A. Pagani, E. Carrera, Unified formulation of geometrically nonlinear refined beam theories, Mech. Adv. Mater. Struct. 25 (2018) 15–31.

[34] M. Filippi, A. Pagani, E. Carrera, Accurate nonlinear dynamics and mode aberration of rotating blades, J. Appl. Mech. 85 (2018) 111004.

[35] L. Cveticanin, Z. Uzelac, Nonlinear longitudinal vibrations of a rod, J. Vib. Control 5 (1999) 827–849.

[36] R. Fernandes, S. El-Borgi, S.M. Mousavi, J.N. Reddy, A. Mechmoum, Nonlinear size-dependent longitudinal vibration of carbon nanotubes embedded in an elastic medium, Physica E 88 (2017) 18–25.
[37] L. Cveticanin, Period of vibration of axially vibrating truly nonlinear rod, J. Sound Vib. 374 (2016) 199–210.
[38] I. Kovacic, M. Zukovic, On the response of some discrete and continuous oscillatory systems with pure cubic nonlinearity: Exact solutions, Internat. J. Non-Linear Mech. 98 (2018) 13–22.
[39] H. Askari, E. Esmailzadeh, D. Younesian, Nonlinear longitudinal vibration solutions of an elastic rod, in: Proceedings of the ASME International Mechanical Engineering Congress and Exposition, Vol. 4B, 2014, pp. V04BT04A027.
[40] J.N. Reddy, An Introduction to the Finite Element Method, third ed., McGraw-Hill, New York, 2006.
[41] S.S. Rao, Vibration of Continuous Systems, John Wiley & Sons, Hoboken, New Jersey, 2007.
[42] J.N. Reddy, An Introduction to Nonlinear Finite Element Analysis, Oxford, UK (2004).
[43] J. Bonet, R.D. Wood, Nonlinear Continuum Mechanics for Finite Element Analysis, second ed., Cambridge University Press, NY, 1997.
[44] A. Föppl, Vorlesungen Uber Technische Mechanik, B. G. Teubner, Leipzig, Germany, 1907, Bd. 5, 132.
[45] T. von Karman, Festigkeitsproblem im maschinenbau, Encyk. D. Math. Wiss. IV (1910) 311–385.
[46] M.W. Hyer, Stress Analysis of Fiber-Reinforced Composite Materials, McGraw-Hill, Boston, 1998.